Proceedings of the 16th International IEEE Annual Conference on Intelligent Transportation Systems (ITSC 2013), The Hague, The Netherlands, October 6-9, 2013

Radar-Based Extended Object Tracking Under Clutter using Generalized Probabilistic Data Association

Christian Adam, Robin Schubert and Gerd Wanielik

***Abstract*— An important foundation for various vehicular applications is a reliable environment recognition. In this context, the simultaneous estimation of the state and the existence of an unknown number of objects under difficult detection conditions is a particular challenge. In this paper, we propose an algorithm for tracking extended objects under clutter. We propose an extended measurement model which enables the estimation of the object width using a standard Kalman filter implementation without the need for clustering the data. As this implies multiple observations generated by one object and additional clutter observations, the generalized probabilistic data association with a state-depended cardinality model is utilized. The proposed algorithm is evaluated with simulated data of a radar-based vehicle tracking system.**

I. Introduction

A large number of advanced driver assistant systems, e. g. adaptive cruise control or active pedestrian safety systems, require knowledge about the objects in the vehicular environment. Based on these information, e. g. position and movement of the objects, decisions like speed adjustment or initiation of an emergency brake can be derived. Usually, cost-effective sensors like radar systems or cameras with downstream object recognition are used for the environment observation. However, these sensors have several weaknesses. One the one hand, not every measurement necessarily belongs to a real existing object. These false-positive measurements, also referred to as *clutter*, whose number is varying over time, have to be identified and eliminated. On the other hand, the sensor could miss an existing object and deliver no measurements. Furthermore, the sensor measurements have a limited resolution and are disturbed by noise.

A commonly used method for overcoming these drawbacks is probabilistic object tracking. Based on noisy measurement data, it estimates the number of objects and the state of each object using a recursive probabilistic filter, e. g. a Kalman filter. One of the major difficulties for multiple object tracking (MOT) is the *data association problem*. Usually, each of the utilized sensors delivers multiple observations. Unfortunately, it is not known a priori which measurements belong to which object or whether a measurement did not originate from an object and, therefore, is clutter. When the objects are spatially extended, i. e. their dimensions are significantly larger than the sensor resolution, multiple observations could be generated by one object.

Christian Adam and Robin Schubert are with the BASELABS GmbH, Ebertstr. 10, 09126 Chemnitz, Germany, e-mail: firstname.lastname@baselabs.de

Gerd Wanielik is with the Professorship of Communications Engineering, Chemnitz University of Technology, Chemnitz, Germany, e-mail: gerd.wanielik@etit.tu-chemnitz.de

In the context of this paper, tracking spatially extended objects means to estimate one or more spatial parameters of an object from multiple measurements, where each individual measurement contains no information about that parameter, but only the whole set of measurements. For example, a radar sensor delivers multiple observations of the rear end of a vehicle. Though non of them contains the quantity *width*, the human observer could easily reconstruct the width by looking at the whole set and drawing a mediating line through the set that ends at the most outer points.

Among others, one way for estimating the spatial as well as the kinematic state of an object is to add the spatial parameters to the state representation as additional quantities. From these, for each observation in the measurement set an according predicted measurement is calculated. Each predicted measurement has a Gaussian distribution which should incorporate the state uncertainties as well as the measurement noise. Due to the Gaussian PDF and the known one-to-one assignment of the measurements, Kalman filter implementations with the capability of sequential updates of multiple measurements can be used for the state update. In [1], the shape and movement of moving objects based on RGB and depth camera has been tracked. In [2], a radar is used to track extended stationary objects like guard rails. These examples have in common, that a probabilistic treatment of clutter is not performed. Thus, clutter that lies inside the gate area can lead to incorrect estimations.

Within this paper, we propose an algorithm that utilizes the general probabilistic data association (GPDA) presented in [3] and [4] for tracking of spatially extended objects under clutter using a radar sensor. By using a proposed extended measurement model, the width can be estimated with a Kalman Filter without any preliminary clustering of the measurements. As this implies that more than one measurement is generated by an object, other probabilistic data association algorithms like IPDA [5] cannot be applied for this problem. The algorithm will be evaluated with simulated data.

The paper is structured as follows: In section II the derivation of the GPDA is presented, followed by the implementation of the algorithm for our tracking problem. The paper closes with an evaluation of the algorithm with simulated data and a conclusion.

II. Generalized Probabilistic Data Association

In this section, the theoretical background of the proposed algorithm is presented. This is a modified version of the derivation we presented in [3]. The following derivation is

978-1-4799-2914-613/$31.00 ©2013 IEEE

given for the case of one single object, as PDA algorithms in contrast to the *joint* variants require a non-probabilistic association of measurements to tracks in order to facilitate an independent calculation for each object.

A typical situation for tracking under clutter is that several measurements $\mathbf{z}^1, \ldots, \mathbf{z}^{n_z} \in \{\mathbf{z}\}$ may potentially have originated from the track $\mathbf{x}$. The measurement set $\{\mathbf{z}\}$ may consist of two subsets $\{\mathbf{z}\}^x$ and $\{\mathbf{z}\}^{\mathrm{cl}}$ which contain the true measurements and the clutter, respectively.

Unfortunately, it is not known which measurements originated from the object and which are clutter. Thus, GPDA defines the set of all possible association hypotheses and represents it by discrete association events $A_i^m \in A^m \subset A$ of a random experiment. The subsets A^m contain all association events A_i^m which are based on the assumption that exactly m measurements have originated from the object. The cardinality of A^m is given by $\binom{n_z}{m}$, where n_z denotes the cardinality of $\{\mathbf{z}\}$. For instance, the event A_1^1 represents the assumption that only $\mathbf{z}^1$ was generated by the object, while A_2^2 assumes that $\mathbf{z}^1$ and $\mathbf{z}^2$ are true measurements. The maximum number of true measurements is either given by n_z or by a predefined system parameter $\overline{n}$.

The derivation of the GPDA equations requires some further notational considerations. The set

$$C_n^k := \left\{ (c_1, c_2, \ldots, c_n) | c_i \in \{0,1\}; \sum_{i=1}^{n} c_i = k \right\} \tag{1}$$

contains all combinations for $n \in \mathbb{N}, k \in \mathbb{N}_0, n \geq k$. For instance, the combinations for drawing two true measurements from a set of three observed ones is given by

$$\begin{aligned} C_3^2 &= \left\{ (c_1, c_2, c_3) | c_i \in \{0,1\}; \sum_{i=1}^{3} c_i = 2 \right\} \\ &= \{(1,1,0), (1,0,1), (0,1,1)\}. \end{aligned} \tag{2}$$

The notation $C_n^k[i,j]$ represents c_j from the ith combination.

A. State Update

The basic idea of GPDA is to condition the probability density function (PDF) of the posterior state on the association events and the existence probability. Thus, from the law of total probability follows

$$\begin{aligned} p(\mathbf{x}_k|\mathbf{Z}_k) = &\sum_{\exists \mathbf{x}} \sum_{A_i^m \in A} \\ &p(\mathbf{x}_k|\mathbf{Z}_k, A_i^m, \exists \mathbf{x}_k)\, P(A_i^m|\mathbf{Z}_k, \exists \mathbf{x}_k)\, P(\exists \mathbf{x}_k|\mathbf{Z}_{k-1}). \end{aligned} \tag{3}$$

Herein, $p(\mathbf{x}_k|\mathbf{Z}_k, A_i^m, \exists \mathbf{x}_k)$ denotes the conditional posterior state PDFs that are determined by the state update of a Bayesian filter (e. g. a Kalman filter) taking all measurements of that association event into account. For their calculations, the track is invariably assumed to exist, therefore, the existence condition can be omitted. If no measurements are generated by the object, the posterior state PDF is equal to the prior state. This is the case either if the object does not exist or for the hypothesis A^0 which assumes all measurements being clutter. With the abbreviation $P_{\mathrm{E}} = P(\exists \mathbf{x}_k = \exists | \mathbf{Z}_{k-1})$ for the prior existence probability, (3) can be rewritten to

$$\begin{aligned} p(\mathbf{x}_k|\mathbf{Z}_k) = &\sum_{A_i^m \in A \setminus A^0} p(\mathbf{x}_k|\mathbf{Z}_k, A_i^m)\, P(A_i^m|\mathbf{Z}_k, \exists \mathbf{x}_k = \exists)\, P_{\mathrm{E}} \\ &+ p(\mathbf{x}_k|\mathbf{Z}_{k-1}) \left(P(A^0|\mathbf{Z}_k, \exists \mathbf{x}_k = \exists)\, P_{\mathrm{E}} + 1 - P_{\mathrm{E}} \right). \end{aligned} \tag{4}$$

For the sake of brevity, we will abbreviate for the rest of the paper the terms $\exists \mathbf{x}_k = \exists$ and $\exists \mathbf{x}_k = \overline{\exists}$ with $\exists_k$ and $\overline{\exists}_k$, respectively. The association probabilities $P(A_i^m|\mathbf{Z}_k, \exists_k)$ need to be calculated separately using Bayes' rule:

$$P(A_i^m|\mathbf{Z}_k, \exists_k) = \eta\, p(\{\mathbf{z}\}_k|A_i^m, \mathbf{Z}_{k-1}, \exists_k)\, P(A_i^m|\mathbf{Z}_{k-1}, \exists_k). \tag{5}$$

We assume that the association probabilities are independent from previous measurements, that is, $P(A_i^m|\mathbf{Z}_{k-1}, \exists_k) = P(A_i^m|\exists_k)$. Furthermore, in default of prior knowledge about the association events, pursuant to the principle of indifference, a uniform distribution is used as their prior probability distribution. Thus, $P(A_i^m|\exists_k)$ cancels out in (4).

The likelihood for the observation of the set $\{\mathbf{z}\}_k$ can be split into several components. As defined previously, the set of measurements consists of the set of true measurements and the set of clutter measurements. Assuming independence between those sets, the likelihood can be written as

$$\begin{aligned} &p(\{\mathbf{z}\}_k|A_i^m, \mathbf{Z}_{k-1}, \exists_k) \\ &\quad = p(\{\mathbf{z}\}_k^x|A_i^m, \mathbf{Z}_{k-1}, \exists_k)\, p(\{\mathbf{z}\}_k^{\mathrm{cl}}|A_i^m, \mathbf{Z}_{k-1}, \exists_k). \end{aligned} \tag{6}$$

Furthermore, by assuming independence between the clutter measurements of different time steps as well as between the clutter and the existence of the object, (6) simplifies to

$$\begin{aligned} &p(\{\mathbf{z}\}_k|A_i^m, \mathbf{Z}_{k-1}, \exists_k) \\ &\qquad = p(\{\mathbf{z}\}_k^x|A_i^m, \mathbf{Z}_{k-1}, \exists_k)\, p(\{\mathbf{z}\}_k^{\mathrm{cl}}|A_i^m). \end{aligned} \tag{7}$$

Each of the two likelihood factors can be split further into a cardinal and a spatial part which are described in the following sections. Again, these parts are assumed to be independent.

1) Spatial Likelihood: The spatial likelihood is defined by the product of the spatial likelihoods for each single measurement. For true measurements, this is $p(\mathbf{z}_k^i|\mathbf{Z}_{k-1}) = \Lambda_k^i$. When a Kalman filter is used for the state update, this value can be obtained by the evaluating the PDF of the predicted measurement $\mathcal{N}(\mathbf{z}, h(\mathbf{x}_k), \mathbf{S}_k)$ at the measurement. However, the likelihood can be represented by an arbitrary PDF as long as it can be evaluated at the measurement. Thus, the spatial likelihood for the subset of true measurements is given by

$$p(\widehat{\{\mathbf{z}\}}_k^x|A_i^m, \mathbf{Z}_{k-1}, \exists_k) = \prod_{j=1}^{n_z} \left(\Lambda_k^i\right)^{C_{n_z}^m[i,j]}. \tag{8}$$

Clutter measurements are assumed to be spatially uniformly distributed over the whole field of vision (FOV) of the sensor. Thus, the overall spatial clutter likelihood is given by

$$p(\widehat{\{\mathbf{z}\}}_k^{\mathrm{cl}}|A_i^m) = V^{-(n_z - m)}, \tag{9}$$

where V denotes the (hyper)volume of the FOV.

978-1-4799-2914-613/$31.00 ©2013 IEEE

2) Cardinal Likelihood: The cardinal likelihood defines the probability of a certain number of true or clutter measurements, respectively, given the association event. While the cardinal clutter likelihood is assumed to be independent from previous time steps, this is not the case for the cardinal likelihood of the true measurements $P(n_x|A_i^m, \mathbf{Z}_{k-1}, \exists_k) = P(n_x)$. The sum of both cardinalities is by definition $n_{\mathrm{cl}} + n_x = n_z$.

In this paper, the clutter cardinality is modeled by a Poisson distribution. Using this distribution is a direct consequence of the assumption that clutter measurements are spatially uniformly distributed over the whole FOV. From the law of small numbers it follows that the number of clutter events inside a relatively small region of the FOV—the gate of the track for instance—follows a Poisson distribution. Its characteristic parameter λ specifies the expectation value of the number of clutter measurements inside a unit hypercube of the FOV. With this parameter, the distribution of the clutter cardinality is given by

$$P(n_{\mathrm{cl}} = k|A_i^m) = \begin{cases} \dfrac{(\lambda V)^{n_z-m}}{(n_z-m)!} e^{-\lambda V} & \text{if } k = n_z - m \\ 0 & \text{else.} \end{cases} \tag{10}$$

Inserting these four likelihood terms in (7) gives

$$p(\{\mathbf{z}\}_k|A_i^m, \mathbf{Z}_{k-1}, \exists_k) = P(n_x = m)\, \frac{\lambda^{n_z-m} e^{-\lambda V}}{(n_z-m)!} \prod_{j=1}^{n_z} \left(\Lambda_k^i\right)^{C_{n_z}^m[i,j]}. \tag{11}$$

3) Association Probabilities: With the above-mentioned considerations the association probabilities can be determined to

$$P(A_i^m|\mathbf{Z}_k, \exists_k) = \frac{1}{1-\delta} P(n_x = m)\, (n_z)^{\underline{m}}\, \lambda^{-m} \prod_{j=1}^{n_z} \left(\Lambda_k^i\right)^{C_{n_z}^m[i,j]}, \tag{12}$$

where the auxiliary variable δ is defined as

$$\delta = 1 - \sum_{m=0}^{\min(\overline{n}, n_z)} P(n_x = m)\, (n_z)^{\underline{m}}\, \lambda^{-m} \sum_{i=1}^{\binom{n_z}{m}} \prod_{j=1}^{n_z} \left(\Lambda_k^i\right)^{C_{n_z}^m[i,j]} \tag{13}$$

and $(n_z)^{\underline{m}}$ denotes the falling factorial, that is,

$$(n_z)^{\underline{m}} = \frac{n_z!}{(n_z-m)!}. \tag{14}$$

B. Existence Update

The GPDA algorithm also requires the update of the existence probability. The derivation of this equation starts by applying Bayes' rule to the required probability distribution:

$$P(\exists \mathbf{x}_k|\mathbf{Z}_k) = \eta\, p(\{\mathbf{z}\}_k|\exists \mathbf{x}_k, \mathbf{Z}_{k-1})\, P(\exists \mathbf{x}_k|\mathbf{Z}_{k-1}). \tag{15}$$

The second term $P(\exists \mathbf{x}_k|\mathbf{Z}_{k-1})$ represents the prior existence probability P_{E}. The likelihood term $p(\{\mathbf{z}\}_k|\exists \mathbf{x}_k, \mathbf{Z}_{k-1})$ is not known in this form and, by analogy to the state update, needs to be conditioned on the association events:

$$p(\{\mathbf{z}\}_k|\exists \mathbf{x}_k, \mathbf{Z}_{k-1}) = \sum_{A_i^m \in A} p(\{\mathbf{z}\}_k|\exists \mathbf{x}_k, A_i^m, \mathbf{Z}_{k-1}) P(A_i^m|\exists \mathbf{x}_k, \mathbf{Z}_{k-1}). \tag{16}$$

Similar to the state update derivation, the prior association probabilities are assumed to be uniformly distributed and are, thus, omitted.

While the measurement likelihood for the case of existence is equal to (11), the complementary case needs to be treated separately. If the object does not exist, every measurement must coercibly be clutter. Thus, this likelihood is given by

$$p(\{\mathbf{z}\}_k|\exists \mathbf{x}_k = \overline{\exists}, A_i^m, \mathbf{Z}_{k-1}) = \begin{cases} \dfrac{\lambda^{n_z}}{n_z!} e^{-\lambda V} & \text{if } i = 0, \\ 0 & \text{else.} \end{cases} \tag{17}$$

With this expression, the final equation for the existence update is

$$P(\exists \mathbf{x}_k = \exists|\mathbf{Z}_k) = \frac{(1-\delta)P_{\mathrm{E}}}{1-\delta P_{\mathrm{E}}}. \tag{18}$$

Due to the binary nature of the distribution, providing the probability for existence is sufficient.

III. Implementation

The proposed algorithm has been evaluated with simulated data. The following section gives a brief description of the object tracking, the models, and the simulation environment.

A. Object Tracking

As the GPDA tracker is a single object tracker (SOT), the tracking component contains one instance of the tracker for each tracked object. Additionally, it performs the measurement association. An unscented Kalman filter (UKF) [6] is used for filtering. For the association events with more than one measurement, a sequential UKF update is performed [7]. For the sake of brevity we omit describing the whole structure, for a detailed description of the tracking steps see [8] and [9]. In the following, only some characteristics of our system are summarized.

Objects are considered to be stick objects, hence, the state space contains the width w as spatial dimension. The other elements of the state space correspond to the CTRV (Constant Turn Rate and Velocity) space [10]:

$$\mathbf{x}_k = \begin{pmatrix} x_k & y_k & \theta_k & v_k & \omega_k & w_k \end{pmatrix}^{\mathrm{T}}. \tag{19}$$

The coordinates x and y represent the center of the line segment. The position and motion elements of the state are propagated through time by a CTRV model [10]. The width is modeled to be constant. Though this is physically correct, a process noise is added. This is necessary to compensate for the inaccurate measurement model (see below). As the object is tracked in the ego vehicle frame, the position and heading are corrected by the ego vehicle movement provided before the state prediction.

978-1-4799-2914-613/$31.00 ©2013 IEEE

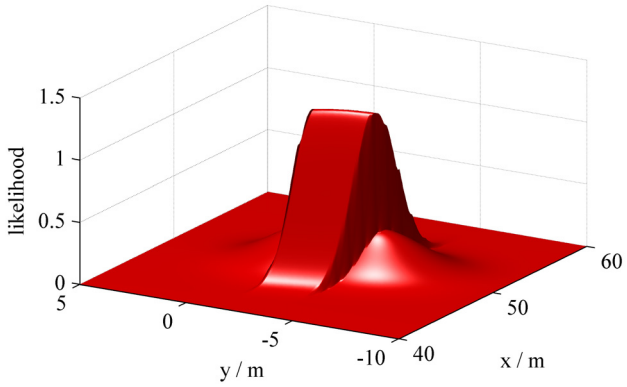

Fig. 1. Example of the spatial measurement likelihood. The track state has the expectation $\mathrm{x} = (50\,\mathrm{m}, -3\,\mathrm{m}, 0.35\,\mathrm{rad}, 0\,\mathrm{m/s}, 0\,\mathrm{rad/s}, 3\,\mathrm{m})^{\mathrm{T}}$ and the covariance matrix $\mathrm{P} = \mathrm{diag}(5, 2.25, 0.03, 10, 0.01, 2)$.

The measurement space consists of the range r, the azimuth φ, and the range rate $\dot{r}$:

$$\mathbf{z}_k = \begin{pmatrix} r_k & \varphi_k & \dot{r}_k \end{pmatrix}^{\mathrm{T}}. \tag{20}$$

For the calculation of the prior existence probability a birth and persistence model is needed [11]. As vehicles cannot disappear as a matter of principle, even if they are outside the FOV, the *persistence probability* is independent from the state and was set to $P_{\mathrm{P}} = 1 - 10^{-10}$. By choosing a value slightly less than unity, the existence of an erroneously created track can decrease. The *birth probability* depends on the prior state of the track. Outside of the FOV it is zero, in its boundary areas is $P_{\mathrm{B}} = 0.95$, and inside is $P_{\mathrm{B}} = 0.01$.

The measurement association assigns each measurement to at most one track. We use the local nearest neighbor approach with gating. Measurements whose Mahalanobis distance to every single track is greater than a threshold are not assigned. The threshold is set according to a gate probability of $P_G = 0.999$, in the three-dimensional case this fits a maximum Mahalanobis distance of $\overline{d} = 4.033$.

New tracks are created from the unassigned measurements. Tracks are deleted either if their existence probability becomes lower than a threshold or if their state covariances have increased too much.

B. Spatial Measurement Likelihood

The spatial measurement likelihood gives the (non-normalized) probability that a measurement $\mathbf{z}_k$ originates from the object with the prior state estimation $p(\mathbf{x}_k|\mathbf{Z}_{k-1})$. For its calculation, the radar coordinates of the projected point $\mathbf{z}_k^{\mathrm{P}}$ are needed which has the same azimuth like the measurement and lies on the line segment of the track. For this, the intersection of the radar beam with the track's line segment is determined by

$$l = \frac{(-y_k + y_{\mathrm{R}})\cos\varphi_k + (x_k - x_{\mathrm{R}})\sin\varphi_k}{\cos(\theta_k - \varphi_k)}, \tag{21}$$

where x_{R} and y_{R} denote the position of the radar in the vehicle frame and l denotes the distance of the intersection

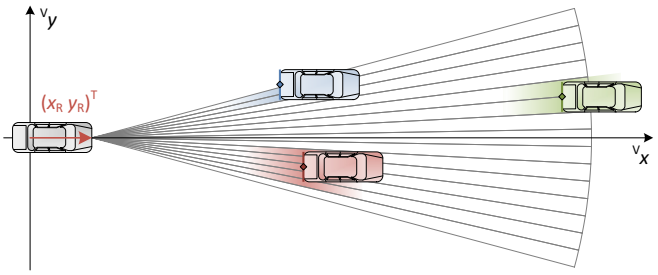

Fig. 2. The cardinality model. The diamonds indicate the estimated position of the tracks, the bars represent the rear surface of the objects. The maximum number of measurements n_{R} is equal to the number of beams that intersect at least partially with the rear surface.

on the track line from the center point. It is limited to the line segment by setting it to $-\frac{w}{2}$ if it is less than this value and to $\frac{w}{2}$ if it is greater, respectively. Thus, measurements lying left or right of the line segment are projected to its endpoints. With the limited value, the radar coordinates including the range rate of $\mathbf{z}_k^{\mathrm{P}}$ are calculated by

$$\mathbf{z}_k^{\mathrm{P}} = \begin{pmatrix} \sqrt{(y_k - y_{\mathrm{R}} + l\cos\theta)^2 + (x_{\mathrm{R}} - x_k + l\sin\theta)^2} \\ -\arctan\frac{y_k - y_{\mathrm{R}} + l\cos\theta}{x_{\mathrm{R}} - x_k + l\sin\theta} \\ v_k\cos(\theta_k - \varphi_k^*) - v_{\mathrm{Ego}}\cos\varphi_k^* \end{pmatrix}., \tag{22}$$

with v_{Ego} denoting the velocity of the ego vehicle. The unscented transformation (UT) [12] is used to transform the Gaussian distribution of the prior state estimation through this nonlinear function into a Gaussian of the projected point. By adding the measurement noise covariance $\mathbf{R}$, the final distribution of the point including all uncertainties is obtained. Finally, the likelihood value is the value of that Gaussian at $\mathbf{z}_k$.

Fig. 1 shows the likelihood function of an exemplary track in the Cartesian plane. The influence of the range rate on the likelihood is not shown, it was set to zero for all measurements.

C. Measurement Cardinality Distribution

The cardinality distribution of the true measurements gives the probability that an object generates n_x measurements given it exists. This number can depend on the state of the object. For instance, when a radar sensor is used, a more distant vehicle appears under a lower visual angle than a nearer one, thus, the farther vehicle is detected by less radar beams. Formally, the cardinality distribution is $P(n_x|A_i^m, \mathbf{x}_k, \exists_k)$.

Like the spatial measurement model, the cardinality model treats the surface of the objects as reflection face with the width specified by the state. It is outlined in fig. 2. The distribution is independent from the association event, that is, $P(n_x|A_i^m, \mathbf{x}_k, \exists_k) = P(n_x|\mathbf{x}_k, \exists_k)$.

For the calculation the coordinates of the endpoints are transformed into the polar radar coordinate system. If the distance of one of the points is greater than the visual range of the sensor or if both points are outside the FOV on the left

978-1-4799-2914-613/$31.00 ©2013 IEEE

or the right side, respectively, the object cannot be detected. In this case, the cardinality distribution is given by

$$P(n_x|\mathbf{x}_k, \exists_k) = \begin{cases} 1 & \text{if } n_x = 0, \\ 0 & \text{else.} \end{cases} \tag{23}$$

If at least one of the points is inside the FOV, the number of radar beams n_R that can perceive the object is calculated. At this, also those beams are included that hit the surface only partially. The probability that the reflected beam actually generates a measurement is denoted by the detection probability P_D. It is multiplied with the probability P_G that the measurement lies inside the gating area around the track. Assuming that these values are constant and independent for each radar beam, the cardinality is given by the binomial distribution

$$P(n_x|\mathbf{x}_k, \exists_k) = \binom{n_\mathrm{R}}{n_x} (P_\mathrm{D} P_\mathrm{G})^{n_x} (1 - P_\mathrm{D} P_\mathrm{G})^{n_\mathrm{R} - n_x}. \tag{24}$$

This distribution is conditioned on a certain instance of the state, while for (12) the probability conditioned on all previous measurements is needed. It can be obtained by evaluating the Chapman-Kolmogorov equation:

$$P(n_x|\mathbf{Z}_{k-1}, \exists_k) = \int P(n_x|\mathbf{x}_k, \exists_k)\, p(\mathbf{x}_k|\mathbf{Z}_{k-1}, \exists_k)\, \mathrm{d}\mathbf{x}_k. \tag{25}$$

No closed-form solution exists for this integral. An approximate solution is obtained by creating a finite set of random samples out of the prior state PDF. Hence, the integral degenerates to a sum (Monte Carlo method). For this paper, we used 100 samples. The same method is applied for the calculation of the birth and persistence probabilities. However, for time-critical applications a further approximation by just using the expectation of the prior state may be sufficient.

D. Measurement Prediction

As an UKF is used for the state update, for each measurement in the association event $\mathbf{z}_k$ a predicted measurement PDF $\mathcal{N}(\mathbf{z}_k^*, \hat{\mathbf{z}}_k^*, \mathbf{S})$ is needed. This is provided by the measurement model.[1] If only one measurement has been assigned to the track at all or if the azimuths of all measurements are equal, the predicted measurement is

$$\mathbf{z}_k^* = \mathbf{h}(\mathbf{x}_k) = \begin{pmatrix} \sqrt{(x_k - x_R)^2 + (y_k - y_R)^2} \\ \arctan \frac{y_k - y_R}{x_k - x_R} \\ v_k \cos(\theta_k - \varphi_k^*) - v_\mathrm{Ego} \cos(\varphi_k^*) \end{pmatrix}. \tag{26}$$

In the case of multiple assigned measurements with at least two different azimuths, the most left and the most right azimuth are stored in φ_L and φ_R, respectively. For both, the intersection with the track line is calculated by (21); the resulting values are l_L and l_R. The position of the intersection of $\mathbf{z}_k$ is also calculated and will be denoted by l.

[1]One could come up with the idea of using the PDF of $\mathbf{z}_k^\mathrm{P}$ provided by the spatial measurement likelihood in (22) as the predicted measurement. Actually, this would cause the width to grow if the set of measurements is more spread than the track width, but, however, it would never shrink in the converse case.

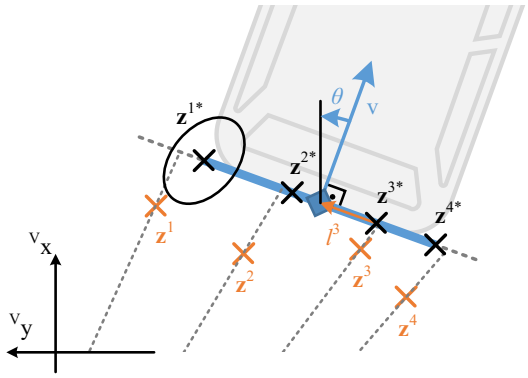

Fig. 3. The extended measurement model. The orange crosses depict the four associated measurements, the thick blue line represents the track line segment. The predicted measurements are depicted by the black crosses. The most outer ones lie on the end points of the line segment, the others are arranged between them. Exemplarily, the value l for $\mathbf{z}^3$ and the covariance ellipse of $\mathbf{z}^{1*}$ are adumbrated.

The model assumes that the most left and right assigned measurements have originated from the end points of the line, thus, their predictions coincide with the end points. The predictions for the remaining measurements are arranged between them with distances proportional to the distances of the projected points of the measurements (fig. 3). This is achieved by a linear transformation of l by

$$l_\mathrm{tr} = \frac{w_k}{l_\mathrm{L} - l_\mathrm{R}} l - \frac{w_k (l_\mathrm{L} + l_\mathrm{R})}{2(l_\mathrm{L} - l_\mathrm{R})}. \tag{27}$$

The predicted measurement is calculated by inserting this value in (22). Like for the measurement likelihood, the covariance of the predicted measurement is the sum of the measurement noise and the covariance obtained by the UT of the state.

If parts of the object are outside the FOV, the model assumption is considerably violated. For instance, if the left half is outside the FOV, a measurement from the center of the object would be matched to left end point. Hence, the UKF would reduce the width and pull the center point to the right. If the object has been detected by the most left or most right radar beam, there is a high probability that parts of the object are not visible. In these cases, a predefined and constant object width $\widetilde{w}$ is assumed. If the track is on the left side of the FOV, l_L is not calculated from the most left measurement, but by

$$l_\mathrm{L} = l_\mathrm{R} + \widetilde{w}. \tag{28}$$

Similarly, if the track is on the right side, it is

$$l_\mathrm{R} = l_\mathrm{L} - \widetilde{w}. \tag{29}$$

Finally, $\widetilde{w}$ is used in (27) instead of w_k. Hence, the width from the track state is not used for the measurement prediction and, thus, it is not updated and remains constant. In addition, this prevents the center point of the track from being spuriously pulled to the center of the measurement set. It is recommended to use the same value for $\widetilde{w}$ which is used for track initialization; we set both to 2 m.

978-1-4799-2914-613/$31.00 ©2013 IEEE

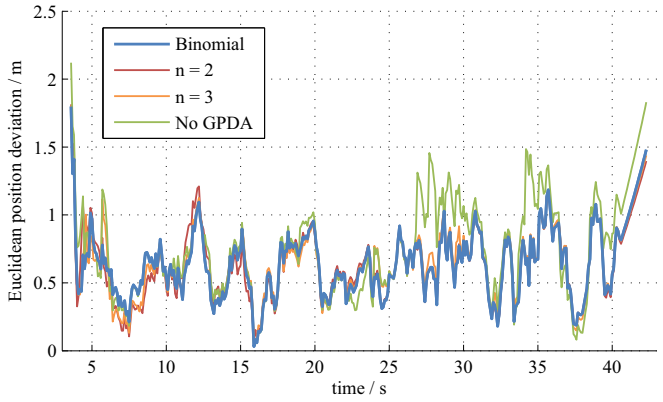

Fig. 4. Euclidean deviation between estimated and true position in the low clutter scenario with $\lambda = 0.01$.

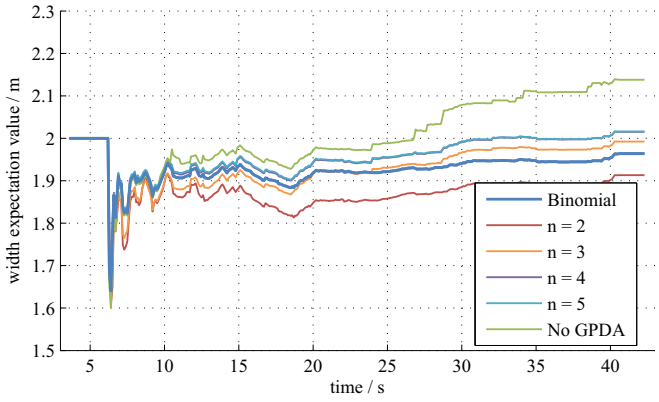

Fig. 5. Evolution of the estimated expectation of the width in the low clutter scenario with $\lambda = 0.01$.

E. Simulation

The proposed algorithm has been evaluated with simulated data. For this, the simulation generates measurements of a single vehicle that passes the ego vehicle on the left side with a relative speed of 5 m/s and a lateral distance of 1.75 m. The time interval between two measurements is 100 ms. The characteristics of the simulated sensor are geared to a long range radar that is commonly used in automotive industries. Its characteristics are summarized in tab. I.

Using the algorithm of the measurement cardinality model the number radar beams that detect the rear side of the vehicle is calculated. The true measurements are calculated using the measurement model in (26). Zero-mean Gaussian noise is added to the measurements in order to simulate the sensor's uncertainties. The measurement is added to the measurement set with a probability of $P_{\mathrm{D}} = 0.9$. The clutter measurements are drawn from a uniform distribution over the whole FOV. The clutter count is set to a fixed value. It is given by

$$n_{\mathrm{cl}} = V_{\mathrm{FOV}}\,\lambda, \tag{30}$$

where λ is the parameter of the intended Poisson distribution and V_{FOV} denotes the hypervolume of the FOV.

Both real and clutter measurements are concatenated to one set and provided to several GPDA trackers with different configurations. As other probabilistic data association algorithms like SPRT and IPDA assume objects to be points and, therefore, cannot be used to estimate the width of an object directly without a pseudo-measurement of the width, the algorithm is evaluated against other variants of the GPDA algorithm. One tracker uses all algorithmic parts presented in this paper including the binomial measurement cardinality. Four trackers use a simple uniform distribution for the measurement cardinality that has been proposed in [3]. They have a limited maximum number of measurements $\overline{n}$ of 2, 3, 4, and 5. Additionally, one tracker uses only the association hypothesis with all assigned measurements, thus, it does not use the GPDA algorithm at all, but only the extended measurement model.

TABLE I
CHARACTERISTICS OF THE SIMULATED RADAR SENSOR

Value	Unit	Range	Accuracy
Range	m	2–150	1.0
Field of view	deg	± 7.5	0.5
Range rate	m/s	± 55	0.75

IV. Simulative Results

A. Low Clutter Scenario with Correct Width

For this evaluation, the clutter cardinality was set to $\lambda = 0.01$. The simulated object width was set to the same value that is used for the track initialization, that is $\widetilde{w} = 2\,m$. Fig. 4 exemplarily shows the tracking results of the position for the GPDA trackers with binomial measurement cardinality, uniform cardinality with $\overline{n} = 2$ and 3 and the tracker without association hypotheses. For the sake of clarity the results for $\overline{n} = 3$ and 4 are omitted.

In most cases, the position estimated by the GPDA trackers is closer to the ground truth than the one of the tracker without any association hypotheses. Especially in the last third, where the object is farther away, GPDA shows significantly better results. However, the binomial measurement cardinality shows a similar performance for the position estimation like the uniform cardinality. This is summarized in the first part of tab. II, where the RMSE values of all estimated quantities are compared. The performances are similar for all values.

The evolution of the expectation value of the width is depicted in fig. 5. It is clearly visible that the width remains constant for the first seconds. This is the expected behavior, because the most left radar beam observes the object in this period. At $t = 6.5\,s$ the most left beam no longer detects the object, thus, the width is estimated from that point on. By chance, one of the end point detections of the object is missing at this time. That causes all filters to estimate a smaller width. Due to the large initial variance of the width, this is corrected after a short time. While the tracker without GPDA overestimates the width, the other ones slowly approach to the true width.

Fig. 6 shows the evolution of the existence probability. The values are provided in log odds . The last column of tab. II

978-1-4799-2914-613/$31.00 ©2013 IEEE

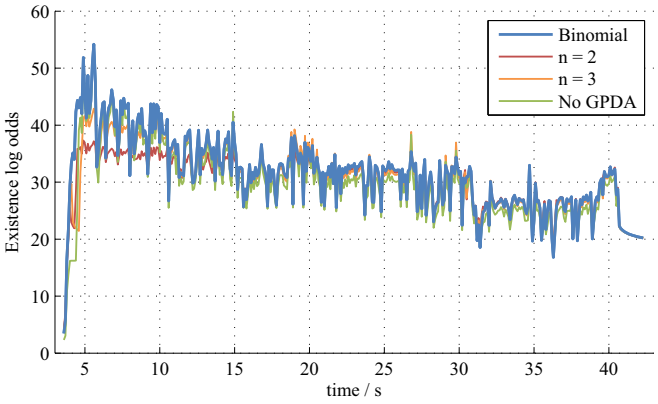

Fig. 6. Evolution of the existence probability in log odds in the low clutter scenario with $\lambda = 0.01$.

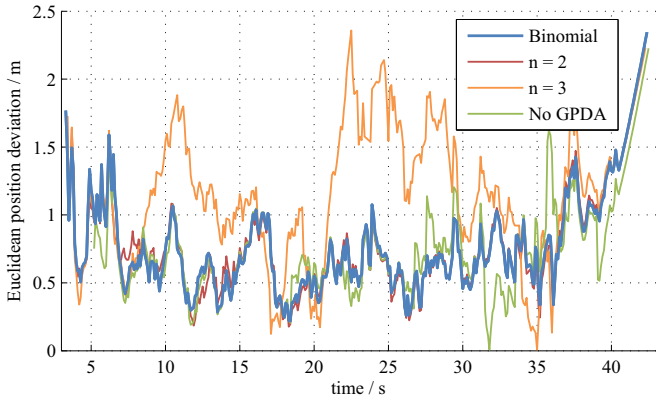

Fig. 7. Euclidean deviation between estimated and true position in the low clutter scenario with $\lambda = 0.01$ and an object width of $w = 2.5\,m$.

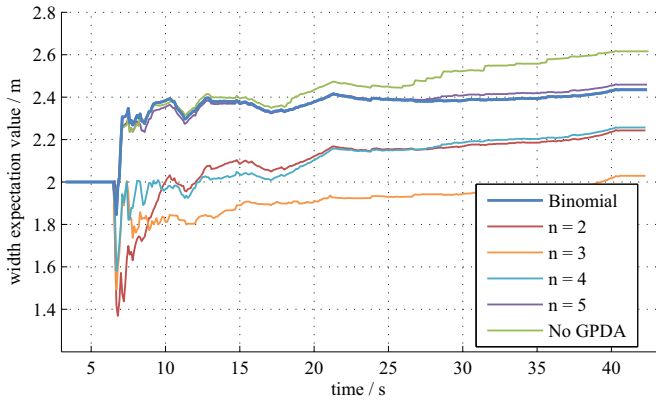

Fig. 8. Evolution of the estimated expectation of the width in the low clutter scenario with $\lambda = 0.01$ and an object width of $w = 2.5\,m$.

contains the mean log odds values for the whole sequence. Log odds are defined by $l = \ln \frac{P_E}{1-P_E}$. The GPDA with binomial cardinality has the steepest slope of the existence and has the greatest existence probability for most of the time. Thus, applications which use the tracking data for making decisions get a more reliable estimation faster than with the other methods. It is noticeable that the existence decreases during the simulation. The reason is that the lateral uncertainty rises due to the limited angular resolution of the radar. Thus, the measurement likelihood values also decrease, which leads to a increasing likelihood that measurements are clutter.

B. High Clutter Scenario with Correct Width

This scenario is similar to the previous one but with $\lambda = 0.05$. The RMSE values of the state quantities and the log odds are summarized in the second part of tab. II. For the position, the velocity, and the yaw rate all trackers using GPDA show similar deviations from the ground truth. For the heading, the uniform cardinality shows even better results. However, the binomial cardinality enables a more accurate width estimation. Without GPDA the state estimation has larger errors except for the width. Like in the previous scenario, the binomial cardinality has the greatest existence probability of all trackers.

C. Low Clutter Scenario with Large Width

For the last scenario, the clutter has been set to $\lambda = 0.01$ again. The width of the simulated object has been changed to $w = 2.5\,m$, but the initial width of the trackers remained $\widetilde{w} = 2\,m$. This corresponds to the common width of trucks. The results of this simulation are summarized in the third part of tab. II. Like in the other scenarios, the proposed GPDA with binomial cardinality has the greatest mean existence probability.

The euclidean position deviation is depicted in fig. 7. The uniform cardinality with $\overline{n} = 3$ shows a significant deviation from the ground truth. The other filters behave more or less similar to the first scenario, but all of them with a greater deviation in comparison to the first scenario with $w = 2\,m$. The uniform cardinality with $\overline{n} = 5$ shows the best performance of all uniform trackers and is comparable to the binomial version.

Fig. 8 shows the evolution of the estimated width. Like expected, the width remains constant at 2 m for the first seconds. When the object has completely entered the FOV, the estimation of the binomial GPDA increases rapidly to a value of 2.3 m and levels out to 2.4 m. Due to the limited angular resolution of the radar, the estimation of the width at large distances can hardly be more accurate than tens of centimeters. It seems like the tracker without GPDA provides a better estimation, but this is only an effect of the overestimating behavior of that tracker known from the first scenario. The uniform trackers are not able to compensate the model violation quick enough and remain at the false widths. The deviating width estimation of the tracker with $\overline{n} = 3$ leads to the error in its position estimation.

V. Conclusions

In this paper, a method for tracking extended objects under clutter has been proposed. By using the proposed extended measurement model, the UKF as an implementation of the Kalman filter can be used for the state estimation. Nor clustering of the measurements neither the calculation of a pseudo-measurement for the width is necessary. The model also accounts for the limited visibility of the vehicles at the

978-1-4799-2914-613/$31.00 ©2013 IEEE

TABLE II

RMSE BETWEEN TRACK STATE AND GROUND TRUTH AND MEAN EXISTENCE LOG ODDS FOR DIFFERENT SIMULATION PARAMETERS.

	Position m	θ rad	v m/s	ω rad/s	w m	log odds
	$\lambda = 0.01,\ w = 2\,m$					
binomial	0.690	0.0619	0.327	0.0259	0.0794	31.3
$\overline{n} = 2$	0.691	0.0655	0.324	0.0165	0.130	29.9
$\overline{n} = 3$	0.697	0.0791	0.325	0.0325	0.0842	30.4
$\overline{n} = 4$	0.703	0.0710	0.328	0.0270	0.0629	30.5
$\overline{n} = 5$	0.707	0.0685	0.329	0.0208	0.0606	30.5
no GPDA	0.830	0.0856	0.363	0.0417	0.0847	29.6
	$\lambda = 0.05,\ w = 2\,m$					
binomial	0.865	0.107	0.469	0.0393	0.0687	28.4
$\overline{n} = 2$	0.889	0.0528	0.331	0.0161	0.112	27.7
$\overline{n} = 3$	0.813	0.0561	0.324	0.0150	0.0895	28.2
$\overline{n} = 4$	0.853	0.0622	0.435	0.0182	0.109	27.9
$\overline{n} = 5$	0.858	0.100	0.377	0.0474	0.119	27.9
no GPDA	1.34	0.0879	0.366	0.0264	0.504	27.1
	$\lambda = 0.01,\ w = 2.5\,m$					
binomial	0.858	0.0657	0.333	0.0384	0.195	33.1
$\overline{n} = 2$	0.852	0.0622	0.321	0.0312	0.430	31.0
$\overline{n} = 3$	1.25	0.0768	0.486	0.0367	0.580	27.6
$\overline{n} = 4$	0.851	0.0693	0.338	0.0379	0.409	31.4
$\overline{n} = 5$	0.847	0.0675	0.338	0.0375	0.194	31.6
no GPDA	1.34	0.0879	0.366	0.0264	0.504	27.1

boundaries of the radar's FOV. The GPDA algorithm enables to model the generation of multiple measurements by one object and additional clutter.

The algorithm has been evaluated with simulated data against previously published variants of the GPDA and a tracker which uses the extended model, but not GPDA for hypothesis generation. Although the simpler methods show performances similar to the proposed algorithm in particular simulation scenarios, the comparable method varies between the scenarios. The proposed GPDA with binomial cardinality shows a well-balanced behavior among all simulations and can handle model violations best. In all simulations, the proposed algorithm shows the most stable existence estimation.

Subject of future work on this topic will be overcoming the strict and immutable association of measurements to the tracks, which is still needed for GPDA. For this, a joint variant of GPDA which performs the probabilistic association over all objects and measurements will be derived.

REFERENCES

[1] M. Baum, F. Faion, and U. Hanebeck, "Tracking ground moving extended objects using rgbd data," in *Multisensor Fusion and Integration for Intelligent Systems (MFI), 2012 IEEE Conference on*, 2012, pp. 186–191.

[2] C. Lundquist, U. Orguner, and F. Gustafsson, "Extended target tracking using polynomials with applications to road-map estimation," *Signal Processing, IEEE Transactions on*, vol. 59, no. 1, pp. 15–26, 2011.

[3] R. Schubert, C. Adam, E. Richter, S. Bauer, H. Lietz, and G. Wanielik, "Generalized probabilistic data association for vehicle tracking under clutter," in *Intelligent Vehicles Symposium (IV), 2012 IEEE*, 2012, pp. 962–968.

[4] C. Adam, R. Schubert, E. Richter, and G. Wanielik, "Generalisierte probabilistische Datenassoziation mit zustandsabhängiger Kardinalitätsverteilung," in *8. Workshop Fahrerassistenzsysteme FAS2012*, Walting im Altmühltal, September 2012, pp. 47–56.

[5] D. Musicki, R. Evans, and S. Stankovic, "Integrated probabilistic data association (ipda)," in *Decision and Control, 1992., Proceedings of the 31st IEEE Conference on*, 1992, pp. 3796–3798 vol.4.

[6] S. Julier and J. Uhlmann, "Unscented filtering and nonlinear estimation," *Proceedings of the IEEE*, vol. 92, no. 3, pp. 401–422, 2004.

[7] C. McManus and T. Barfoot, "A serial approach to handling high-dimensional measurements in the sigma-point kalman filter," in *Proceedings of Robotics: Science and Systems*, Los Angeles, CA, USA, June 2011.

[8] R. Schubert, *Integrated Bayesian Object and Situation Assessment for Lane Change Assistance*. Aachen: Shaker, 2011.

[9] E. Richter, *Non-Parametric Bayesian Filtering for Multiple Object Tracking*. Aachen: Shaker, 2012.

[10] R. Schubert, C. Adam, M. Obst, N. Mattern, V. Leonhardt, and G. Wanielik, "Empirical evaluation of vehicular models for ego motion estimation," in *Intelligent Vehicles Symposium (IV), 2011 IEEE*, 2011, pp. 534–539.

[11] M. Maehlisch, W. Ritter, and K. Dietmayer, "De-cluttering with integrated probabilistic data association for multisensor multitarget acc vehicle tracking," in *Intelligent Vehicles Symposium, 2007 IEEE*, 2007, pp. 178–183.

[12] S. Julier, "The scaled unscented transformation," in *Proceedings of the American Control Conference*, vol. 6, 2002, pp. 4555–4559 vol.6.

978-1-4799-2914-613/$31.00 ©2013 IEEE